Наносистеми, наноматеріали, нанотехнології
Nanosistemi, Nanomateriali, Nanotehnologii
2020, т. 18, № 2, сс. 333–344

PACS numbers: 06.60.Vz, 42.62.Cf, 81.07.-b, 81.20.Vj, 81.40.Np, 81.70.Bt, 89.20.Bb

Nanoscale Structures of Laser–Arc Welded Joints of High-Strength Low-Alloy Steels

O. M. Berdnikova, A. V. Bernatskyi, V. D. Pozniakov, T. O. Alekseienko, V. M. Sydorets, and O. I. Bushma

E. O. Paton Electric Welding Institute, N.A.S. of Ukraine,
11, Kazimir Malevich Str.,
UA-03150 Kyiv, Ukraine

Low-alloyed high-strength steels with a yield strength of above 600 MPa are widely used for the manufacture of various types of critical-purpose constructions (freight cars, bridges, pressure vessels, truck bodies of lorries, parts of load-lifting cranes, pipelines, ship hulls, etc.). Arc welding of these steels cannot satisfy the industry due to both the low productivity and the need for a heat treatment before or after welding. Without heat treatment, cold cracks form in these steels in the overheating area or in the weld where the metal is quenched during welding, and softening zones appear in the heat-affected zone outside the quenching sites. The hybrid laser–arc welding is becoming more common in the industry. This is due to the prospect of introducing hybrid laser–arc welding instead of arc processes, since such a replacement does not require a relatively large expenditure on the re-training of production and provides a noticeable increase in productivity. At the same time, a significant part of the thermal power required to melt the metal in hybrid laser–arc welding is provided by the use of cheap arc power sources. Previously, the authors determined the optimal speed of hybrid laser–arc welding from the point of view of the phase composition of the structural components, dispersion of the grain structure, the proportion of brittle fracture, etc. However, it was not clear, what effect of the dislocation structure is on the crack resistance measure—fracture toughness. The aim of this paper is to study the effect of external bending load on the dislocation structure and on fracture toughness of low-alloyed high-strength steel welded joints produced by hybrid laser–arc welding by the mode at optimum welding rate. The structural factors, which guarantee a high level of strength and crack resistance of welded joints of high-strength steel, are identified. As shown, the complex of properties of welded joints under external loading in a wide range of temperature conditions ensures the formation of fragmented lower bainite structure with a uniform distribution of the dislocation density and nanoparticles of carbide phases.

Низьколеґовані високоміцні сталі з межею плинности понад 600 МПа широко використовуються для виготовлення різного типу конструкцій відповідального призначення (вантажні вагони, мости, судини під тиском, кузова вантажних автомобілів, деталі вантажопідіймальних кранів, трубопроводи, корпуси суден тощо). Дугове зварювання цих сталей не може задовольнити промисловість через низьку продуктивність і необхідність термічного оброблення до або після зварювання. Без термооброблення у цих сталях утворюються холодні тріщини у зоні перегріву або у звареному шві, де метал гартується під час зварювання, і в зоні термічного впливу поза зонами загартування, де з'являються зони розм'якшення. Гібридне лазерно-дугове зварювання стає все більш поширеним у промисловості. Це пов'язане з перспективою впровадження гібридного лазерно-дугового зварювання замість дугових процесів, оскільки така заміна не вимагає великих витрат на переобладнання виробництва та забезпечує помітне збільшення продуктивности. У той же час значна частина теплової енергії, потрібної для топлення металу при гібридному лазерно-дуговому зварюванні, забезпечується використанням дешевих джерел живлення дуги. Раніше автори визначили оптимальну швидкість гібридного лазерно-дугового зварювання з точки зору фазового складу структурних складових, дисперґування зеренної структури, частки крихкого руйнування та ін. Однак неясно, який вплив мають дислокаційні структури на показник тріщиностійкости — в'язкість руйнування. Метою даної роботи було вивчення впливу зовнішнього згинального навантаження на дислокаційну структуру та на тріщиностійкість зварних з'єднань з низьколеґованої високоміцної сталі, одержаних гібридним лазерно-дуговим зварюванням в режимі з оптимальною швидкістю зварювання. Визначено структурні чинники, що ґарантують високий рівень міцности та тріщиностійкости зварних з'єднань високоміцної сталі. Показано, що комплекс властивостей зварних з'єднань при зовнішньому навантаженні в широкому інтервалі температурних умов забезпечує формування фраґментованої структури нижнього бейниту з рівномірним розподілом густини дислокацій і наночастинок карбідних фаз.

Низколегированные высокопрочные стали с пределом текучести более 600 МПа широко используются для изготовления различного типа конструкций ответственного назначения (грузовые вагоны, мосты, сосуды под давлением, кузова грузовых автомобилей, детали грузоподъёмных кранов, трубопроводы, корпуса судов и т.д.). Дуговая сварка этих сталей не может удовлетворить промышленность из-за низкой производительности и необходимости термической обработки до или после сварки. Без термообработки в этих сталях образуются холодные трещины в зоне перегрева или в сварном шве, где металл закаливается во время сварки, и в зоне термического влияния вне зон закалки, где появляются зоны размягчения. Гибридная лазерно-дуговая сварка становится всё более распространённой в промышленности. Это связано с перспективой внедрения гибридной лазерно-дуговой сварки вместо дуговых процессов, поскольку такая замена не требует относительно больших затрат на переоборудование производства и обеспечивает заметное увеличение производительности. В то же время значительная часть тепловой

энергии, необходимой для плавления металла при гибридной лазерно-дуговой сварке, обеспечивается использованием дешёвых источников питания дуги. Ранее авторы определили оптимальную скорость гибридной лазерно-дуговой сварки с точки зрения фазового состава структурных составляющих, диспергирования зёренной структуры, доли хрупкого разрушения и др. Однако неясно, какое влияние имеют дислокационные структуры на показатель трещиностойкости — вязкость разрушения. Целью работы было изучение влияния внешней изгибающей нагрузки на дислокационную структуру и на трещиностойкость сварных соединений из низколегированной высокопрочной стали, полученных гибридной лазерно-дуговой сваркой в режиме с оптимальной скоростью сварки. Определены структурные факторы, гарантирующие высокий уровень прочности и трещиностойкости сварных соединений высокопрочной стали. Показано, что комплекс свойств сварных соединений при внешнем нагружении в широком интервале температурных условий обеспечивает формирование фрагментированной структуры нижнего бейнита с равномерным распределением плотности дислокаций и наночастиц карбидных фаз.

Key words: low-alloyed high-strength steel, hybrid laser–arc welding, structure–phase composition, nanoscale structures, dislocation density, crack growth resistance.

Ключові слова: низьколеґована високоміцна сталь, гібридна лазерно-дугове зварювання, структурно-фазовий склад, нанорозмірні структури, густина дислокацій, тріщиностійкість.

Ключевые слова: низколегированная высокопрочная сталь, гибридная лазерно-дуговая сварка, структурно-фазовый состав, наноразмерные структуры, плотность дислокаций, трещиностойкость.

(Received 12 December, 2019)

1. INTRODUCTION

Low-alloyed high-strength steels with a yield strength of above 600 MPa are widely used for the manufacture of various types of critical-purpose items (freight cars, bridges, pressure vessels, truck bodies of lorries, parts of load-lifting cranes, pipelines, ship hulls, *etc.*) [1–6]. To increase the service properties and reduce consumption of metal and weight, these structures are manufactured from high-strength low-alloyed steels. Their welding is mainly carried out by arc methods [1, 3, 5]. Proper efficiency of welded products is achieved by ensuring the quality formation of welded joints. Heat treatment at the stages of production of steel and workpieces, before welding individual components or after welding a product is very important. However, it depends on the production capacity and the cost of the heat treatment itself [1, 3].

A special feature of welding of low-alloyed high-strength steels is their sensitivity to overheating with deterioration of the metal properties of the heat-affected zone (HAZ), the tendency to cold cracks in the overheating area or in the weld where metal hardening occurs during welding, and the occurrence of loss-of-strength zones in the HAZ outside the quench areas [1, 3, 5, 7–11]. Cracking is avoided by slowing down the cooling during welding, performing various kinds of heating, which complicates the technological process and worsens the working conditions of the staff, post-weld heat treatment or using high-alloyed electrode materials [1–3, 12–14]. The last ones are characterized by high cost and negatively affect the environmental friendliness of the process [15, 16].

Finding ways to improve the quality and properties of high-strength steel joints, while ensuring enhanced welding productivity, is an urgent task.

The hybrid laser–arc welding is becoming more common in the industry [5, 7, 9, 14, 17–19]. Analysis [1, 3, 5, 8, 20–25] and commercial inquiries of enterprises indicates the interest of researchers and businessmen in the use of hybrid laser–arc welding for the manufacture of metal structures from high-strength steels with a yield strength $\sigma_T \geq 600$ MPa. This is due to the prospect of introducing hybrid laser–arc welding instead of arc processes. Since such a replacement does not require a relatively large expenditure on the re-training of production, and provides a noticeable increase in productivity. At the same time, a significant part of the thermal power required to melt the metal in hybrid laser–arc welding is provided by the use of cheap arc power sources.

As was shown in [5, 7–9, 14, 17–21], local heat input during hybrid laser–arc welding can lead to the formation of quenching structures in the weld metal and HAZ of welded joints from high-strength steels. This may adversely affect the mechanical properties of welded joints [5, 8, 22, 25]. Nevertheless, it is known that, with this method of welding, residual deformations are less than with arc processes [9, 14, 21, 23].

It is known that the mechanical properties and resistance to the formation of cold cracks in welded joints of low-alloyed high-strength steels are significantly affected by the structure of the weld metal and HAZ of the joints [1, 3, 5, 7–9, 13, 17, 18, 26–30]. At present, the processes of structure formation in the weld metal and HAZ of welded joints during arc welding are studied quite well [31–36]. The effect of the thermal cycle in hybrid laser–arc welding on the structure and properties of the weld metal and the HAZ remains insufficiently studied, since, as a result of the synergistic effect, during such a process, the above parameters can vary significantly.

The formation of joints in the welding process occurs under the influence of many factors, unfortunately not always favourable. This is one of the causes of the formation of defects, namely: deviations of the shape and size of the welds from the design, violations of their continuity due to pores, slag inclusions, cracks, non-fusion, undercuts and the like. Experience shows that even the widespread use of non-destructive testing methods such as x-ray, ultrasonic and magnetic flaw detection do not guarantee the detection of all small and sometimes large defects, which can be a source of nucleation of macrocracks. Since defects are a source of initiation of destruction of welded structures, to ensure the reliability of their operation, it is necessary to understand the nature of the formation and development of cracks from defects under various loading conditions.

The authors [5, 7], using the methods of light and scanning microscopy, carried out the preliminary metallographic studies of the structure and fractographic studies of fractures of welded joints produced by hybrid laser–arc welding at various modes. The fracture surfaces of welded joints obtained by impact bending tests at various temperatures were investigated. The authors concluded which mode is optimal (welding speed 20 mm/s) from point of view of the phase composition of the structural components, dispersion of the grain structure, *etc.* However, it is not clear, what effect the dislocation structure is on the crack resistance measure—fracture toughness.

The aim of this work is to study the effect of external bending load on the dislocation structure and on fracture toughness (K_{1C}) of low-alloyed high-strength steel welded joints produced by hybrid laser–arc welding by the optimum mode at a welding speed of 20 mm/s.

2. EXPERIMENTAL DETAILS

2.1. Technology of Welded Joints Production

Hybrid laser–arc welding of butt joints of high-strength low-alloyed steel NA-XTRA-70 (0.19% C, 0.63% Si, 0.85% Mn, 0.65% Cr, 0.12% Ni, 0.13% Mo; no more than 0.01% S and 0.02% P) 10 mm thick was carried out on samples without bevel edges. For the generation of laser radiation in continuous mode Nd:YAG laser ‘DY044’ manufactured by ‘ROFIN-SINAR’ (Germany) was used. The parameters of welding modes are as follow: laser power—4.4 kW, the depth of focal plane of the lens relative to the surface of the welded samples—1.5 mm, the speed of movement of the heating source—72 m/h (20.0 mm/s), arc current—125 A, arc voltage—23 V. Union NiMoCr solid wire of 1.0 mm diameter was used as the

TABLE 1. Mechanical testing of fracture toughness (K_{1C}) of welded joints.

T_{test}, °C	K_{1C}, MPa·m$^{1/2}$	
	Weld	HAZ
+20	90.8	89.9
–20	87.7	84.9
–40	74.7	70.7

filler material.

2.2. Mechanical Testing

The tests were carried out for the weld bead and HAZ of welded joints at temperatures $T_{test} = +20$°C, –20°C and –40°C. The values of crack resistance, namely, fracture toughness (K_{1C}), are presented in Table 1. From the test results, it can be seen that, at low temperature test ($T_{test} = -40$°C), the value of K_{1C} decreases slightly and, at $T_{test} = -20$°C, almost remains at the level corresponding to $T_{test} = +20$°C.

3. RESULTS AND DISCUSSION

3.1. Fractographic Studies

After testing at $T_{test} = +20$°C (Fig. 1, *a*, *b*) and $T_{test} = -20$°C (Fig. 1, *c*, *d*) of the metal of welded beads and HAZ of welded joints for the microrelief of surface of fracture, the ductile fracture with a size of 1–8 μm of dimples is typical. At $T_{test} = -20$°C, the dimple relief is mixed, *i.e.*, these are dispersed dimples (up to 8 μm) and larger ones (15–45 μm) (Fig. 1, *c*, *d*).

Reducing the temperature of the test to $T_{test} = -40$°C leads to a decrease (up to 70%) of the proportion of the ductile component in the weld metal. The nature of fracture is mixed, *i.e.*, predominantly ductile in combination with transcrystalline quasi-brittle (Fig. 1, *e*). The ductile component contains both dispersed dimple *s* (2–5 μm) and ones with larger sizes (20–50 μm). The size of the quasi-brittle fracture facets is 20–50 μm. For HAZ at $T_{test} = -40$°C, a ductile type of fracture is characterized (Fig. 1, *f*).

Thus, fractographic studies have shown that the weld metal and the HAZ of a welded joint of low-alloyed high-strength steel produced by hybrid laser–arc welding at a speed of 20 mm/s after bending at different temperatures have the nature of predominantly ductile fracture, which evidences about high crack resistance.

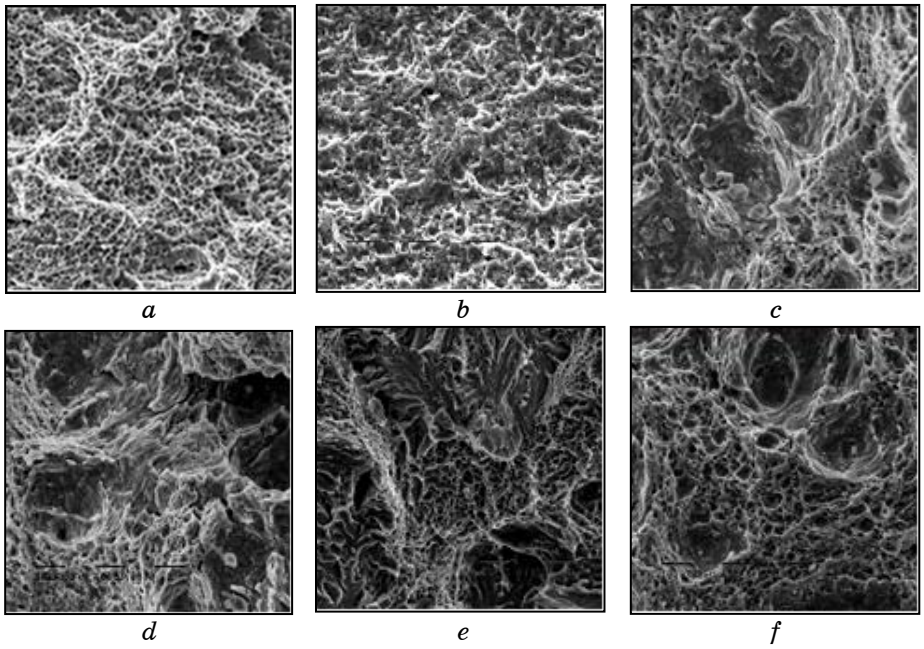

Fig. 1. The microstructure of fracture surface of the weld metal (*a*, *c*, *e*) and HAZ (*b*, *d*, *f*) of welded joints at various test temperatures: (*a*), (*b*) $T_{test} = +20°C$; (*c*), (*d*) $T_{test} = -20°C$; (*e*), (*f*) $T_{test} = -40°C$; ×1550.

3.2. TEM Studies

Further studies were carried out by transmission electron microscopy (TEM) on fracture samples of welded joints obtained at a test temperature of –40°C. The fine structure of the weld metal (Fig. 2) and the HAZ of the welded joint (Fig. 3) was studied in detail: the change in density and distribution of dislocations in the structural components, the nature of the emerging substructure, *etc.*

It is shown that, after loading by bending in the weld metal (Fig. 2) and HAZ (Fig. 3), the substructures of laths of lower (B_L) and upper (B_U) bainite are fractionized to $h_\lambda = 80–300$ nm and $h_l = 130–400$ nm, respectively. The width of the acicular structure of martensite (M) is $h_1 = 170–370$ nm. The lower bainite is formed in the weld (60%) and in the HAZ (80%) with 15–20% martensite. During the transition from the weld to the HAZ, the volume fraction of upper bainite decreases from 20% to 5%.

In the lower bainite, there is a fragmented substructure with clear boundaries of size $d_C = 80–300$ nm (in the weld, Fig. 2, *a*, *b*) and $d_C = 130–400$ nm (in the HAZ, Fig. 3, *a*, *b*) at uniform distribution of dislocation density $\rho = (8–9)\cdot 10^{10}$ см$^{-2}$.

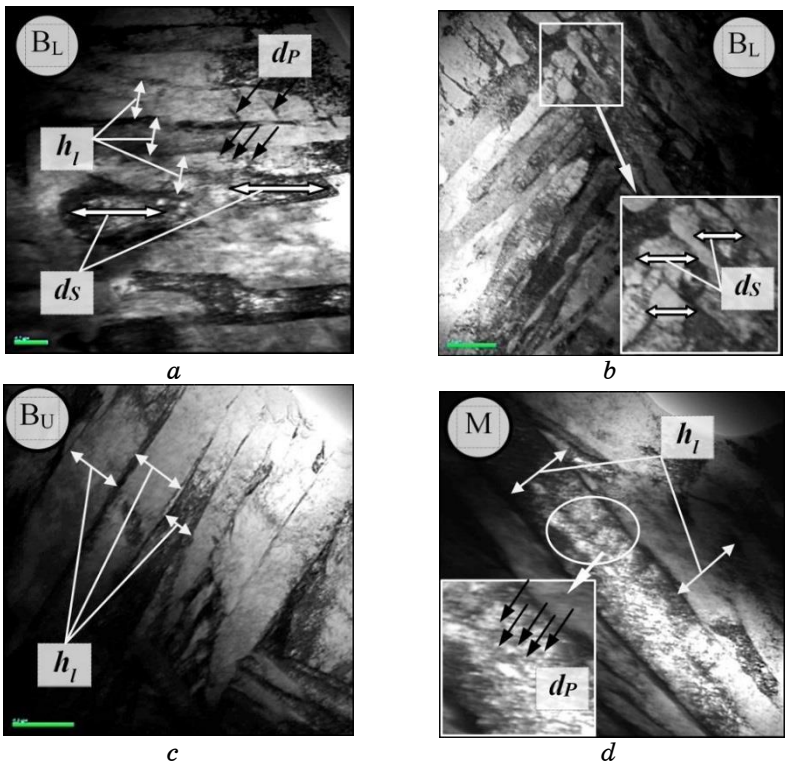

Fig. 2. The fine structure of the weld metal of steel N-A-XTRA-70: (*a*), (*b*) lower bainite (×22000); (*c*) upper bainite (×25000); (*d*) martensite (×35000).

The structure of the upper bainite is characterized by the formation of dislocation clusters along the boundaries with a certain increase in the density of dislocations up to $\rho = 9 \cdot 10^{10}–10^{11}$ cm^{-2} (Fig. 2, *c*; Fig. 3, *c*). In the structure of tempering martensite, the dislocation density uniformly increases in volume of the laths to $\rho = 10^{11}$ cm^{-2} (Fig. 2, *d*; Fig. 3, *d*). In this case, both the structure of the lower bainite and martensite are characterized by the presence of nanoparticles of carbide phases. The sizes of nanoparticles of carbide phases uniformly distributed throughout the bulk of the structural components of the lower bainite and martensite are of 10–30 nm.

Thus, external loading contributes to the fragmentation of the structure of lower bainite with a uniform distribution of the dislocation density and nanoparticles of carbide phases in the structural components of lower bainite and martensite. At the same time, the volume fraction of the upper bainite is insignificant, and the crack resistance of welded joints under external loading in a wide range

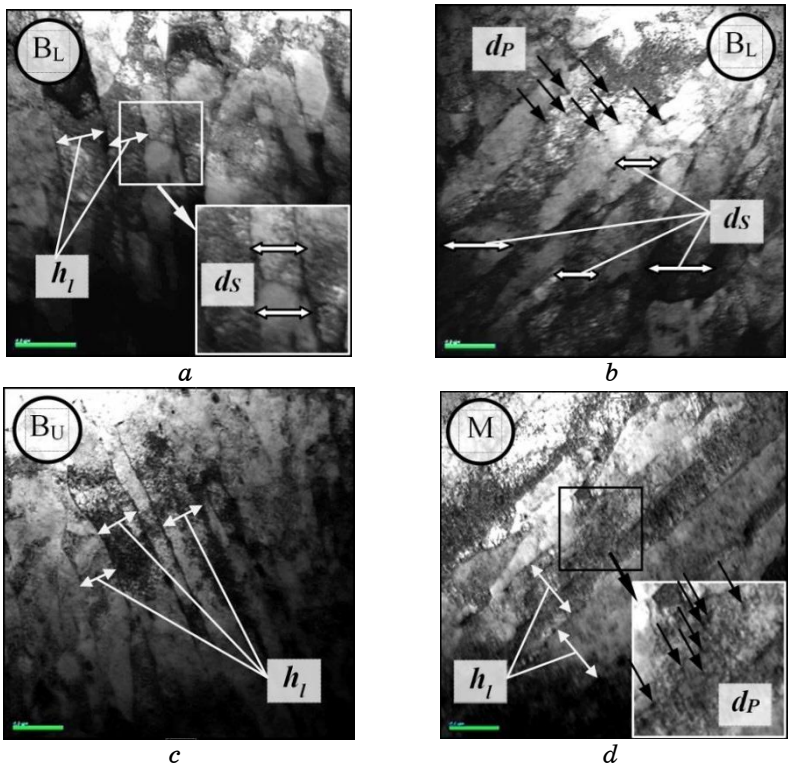

Fig. 3. The fine structure of the HAZ metal of the welded joint of steel N-A-XTRA-70: (*a*), (*b*) lower bainite (×25000); (*c*) upper bainite (×25000); (*d*) martensite (×25000).

of temperature conditions is ensured by the prevalence of the lower bainite structure. This, accordingly, ensures the operational reliability of high-strength steel welded joints N-A-XTRA-70.

3.3. Analytical Evaluation of Structural Hardening

Analytical evaluation of the change in strength (σ_T) of welded joints after external loading (K_{1C}), taking into account the contribution of all structural parameters, was carried out according to the dependences by Hall–Petch, Orowan, *etc*. [8]. The following structural parameters were taken into account: size of subgrains, dislocation density, sizes of carbide phases in structural components and intercarbide distances, volume fraction of structures in the welding zone (in the weld metal and HAZ).

Analytical estimates show that, under the conditions of a welding speed of 20 mm/s in the weld metal and HAZ, the calculated value

TABLE 2. Structural hardening weld metal and HAZ of welded joints.

Hardening			Zone	
			Weld	HAZ
Friction of lattice	σ_0, MPa		20–30	20–30
Solid solution	σ_{SS}, MPa		148	110
Grain	$\Delta\sigma_G$, MPa		91	113
Subgrain	$\Delta\sigma_{SG}$, MPa	B_L	300	400
		B_H	75	19
		M	75	56
Dispersive	$\Delta\sigma_{DH}$, MPa	B_L	173	255
		B_H	12	6
		M	67	30
Dislocation	$\Delta\sigma_{\text{Disl}}$, MPa		195	243
Total	$\Sigma\Delta\sigma_T$, MPa		1161	1259

of hardening is $\Sigma\Delta\sigma_T = 1161–1259$ MPa as presented in Table 2. The highest value of hardening, both in the seam and in the HAZ, is substructural ($\Delta\sigma_{SG} = 450–475$ MPa), dispersive ($\Delta\sigma_{DH} = 252–293$ MPa) and dislocation ($\Delta\sigma_{\text{Disl}} = 195–243$ MPa) hardenings. At the same time, the structure of lower bainite makes the greatest contribution (70–80%) to these components of structural hardening.

Thus, studies have shown that the weld metal produced by hybrid laser–arc welding at a speed of 20 mm/s after external loading at low temperatures has high strength and crack resistance.

4. CONCLUSION

TEM studies have obtained data on the fine structure parameters of lower and upper bainite, martensite: subgrain components, structure fragmentation, and on the distribution of dislocation density in the metal of welded joints of low-alloyed high-strength steel N-A-XTRA-70.

The relationship between the phase composition, structure parameters, fracture toughness and strength of welded joints has been revealed.

The structural factors that guarantee a high level of strength and crack resistance of welded joints of high-strength steel are identified. It is shown that the complex of properties of welded joints under external loading in a wide range of temperature conditions ensures the formation of fragmented lower bainite structure with a uniform distribution of the dislocation density and nanoparticles of carbide phases.

REFERENCES

1. T. K. Roy, Bhattacharya, C. B. Ghosh, and S. K. Ajmani, *Advanced High Strength Steel: Processing and Applications* (Singapore: Springer: 2018); https://doi.org/10.1007/978-981-10-7892-7.
2. S. K. Sharma and S. Maheshwari, *Journal of Natural Gas Science and Engineering*, **38**: 203 (2017); https://doi.org/10.1016/j.jngse. 2016.12.039.
3. J. Villalobos, A. Del-Pozo, B. Campillo, J. Mayen, and S. Serna, *Metals*, **8**, No. 5: 351 (2018); https://doi.org/10.3390/met8050351.
4. R. Oyyaravelu, P. Kuppan, and N. Arivazhagan, *Journal of Advanced Research*, **7**, No. 3: 463 (2016); https://doi.org/10.1016/j.jare.2016.03.005.
5. V. Poznyakov, O. Berdnikova, and O. Bushma, *Materials Science Forum*, **870**: 630 (2016); https://doi.org/10.4028/www.scientific.net/MSF.870.630.
6. J. Zhou, J. Yang, Y. Ye, and G. Dai, *Proc. International Conference on Advanced Technology of Design and Manufacture (November 23–25, 2010)* (Beijing: IET: 2010), p. 28; https://doi.org/10.1049/cp.2010.1254.
7. V. Poznyakov, L. Markashova, O. Berdnikova, and T. Alekseienko, S. Zhdanov, *Materials Science Forum*, **927**: 29 (2018); https://doi.org/10.4028/www.scientific.net/MSF.927.29.
8. L. Markashova, O. Berdnikova, A. Bernatskyi, M. Iurzhenko, and V. Sydorets, *Proc. Young Scientists Forum on Applied Physics and Engineering (October 17–20, 2017)* (Lviv: IEEE: 2017), p. 88; https://doi.org/10.1109/YSF.2017.8126596.
9. B. Acherjee, *Optics & Laser Technology*, **99**: 60 (2018); https://doi.org/10.1016/j.optlastec.2017.09.038.
10. F. Liu, X. Yu, C. Huang, L. He, Y. Chen, and W. Bu, *J. Wuhan Univ. Technology–Mat. Sci. Edit.*, **30**, No. 4: 827 (2015); https://doi.org/10.1007/s11595-015-1236-0.
11. F. Farrokhi, J. Siltanen, and A. Salminen, *Journal of Manufacturing Science and Engineering*, **137**, No. 6: 061012 (2015); https://doi.org/10.1115/1.4030177.
12. M. Rossini, P. R. Spena, L. Cortese, P. Matteis, and D. Firrao, *Materials Science and Engineering: A*, **628**: 288 (2015); https://doi.org/10.1016/j.msea.2015.01.037.
13. M. Sokolov, A. Salminen, E. I. Khlusova, M. M. Pronin, M. Golubeva, and M. Kuznetsov, *Physics Procedia*, **78**: 255 (2015); https://doi.org/10.1016/j.phpro.2015.11.036.
14. X. Cao, P. Wanjara, J. Huang, C. Munro, and A. Nolting, *Materials & Design*, **32**, No. 6: 3399 (2011); https://doi.org/10.1016/j.matdes.2011.02.002.
15. O. G. Levchenko, A. O. Lukianenko, O. V. Demetska, and O. Yu. Arlamov, *Materials Science Forum*, **927**: 86 (2018); https://doi.org/10.4028/www.scientific.net/MSF.927.86.
16. N. Pavlov, A. Kryukov, D. Il'Yaschenko, and D. Chinakhov, *Materials Science Forum*, **906**: 137 (2017); https://doi.org/10.4028/www.scientific.net/MSF.906.137.
17. S. Katayama, *Handbook of Laser Welding Technologies* (Cambridge: Woodhead Publishing Limited: 2013).
18. U. Reisgen, I. Krivtsun, B. Gerhards, and A. Zabirov, *Journal of Laser Applications*, **28**, No. 2: 022402 (2016); https://doi.org/10.2351/1.4944096.
19. V. D. Shelyagin, I. V. Krivtsun, Yu. S. Borisov, V. Yu. Khaskin, T. N. Nabok,

A. V. Siora, A. V. Bernatsky, S. G. Vojnarovich, A. N. Kislitsa, and T. N. Nedej, *Avtomaticheskaya Svarka*, **8**: 49 (2005).
20. I. Krivtsun, U. Reisgen, O. Semenov, and A. Zabirov, *Journal of Laser Applications*, **28**, No. 2: 022406 (2016); https://doi.org/10.2351/1.4943994.
21. M. Rethmeier, S. Gook, M. Lammers, and A. Gumenyuk, *Transactions of JWRI*, **27**, No. 2: 74 (2009); https://doi.org/10.2207/qjjws.27.74s.
22. M. A. Kesse, E. A. Gyasi, and P. Kah, *Proc. the 27th International Ocean and Polar Engineering Conference (June 25–30, 2017)* (San Francisco: International Society of Offshore and Polar Engineers: 2017), p. 42.
23. F. Mirakhorli, X. Cao, X. T. Pham, P. Wanjara, and J. L. Fihey, *Materials Science Forum*, **879**: 1305 (2017); https://doi.org/10.4028/www.scientific.net/MSF.879.1305.
24. F. Farrokhi, R. M. Larsen, and M. Kristiansen, **89**: 49 (2017); https://doi.org/10.1016/j.phpro.2017.08.019.
25. X. Cao, P. Wanjara, J. Huang, C. Munro, and A. Nolting, *Materials & Design*, **32**, No. 6: 3399 (2011); https://doi.org/10.1016/j.matdes.2011.02.002.
26. A. Kurc-Lisiecka and A. Lisiecki, *Materiali in Tehnologije*, **51**, No. 7: 199 (2017); https://doi.org/0.1515/amm-2017-0253.
27. W. Guo, J. A. Francis, L. Li, A. N. Vasileiou, D. Crowther, and A. Thompson, *Materials Science and Technology*, **32**, No. 14: 1449 (2016); https://doi.org/10.1080/02670836.2016.1175687.
28. L. Markashova, O. Berdnikova, T. Alekseienko, A. Bernatskyi, and V. Sydorets, *Advances in Thin Films, Nanostructured Materials, and Coatings* (Eds. A. D. Pogrebnjak and V. Novosad) (Singapore: Springer: 2019), p. 119; https://doi.org/10.1007/978-981-13-6133-3_12.
29. V. Yerofeyev, R. Logvinov, V. Nesterenkov, and A. Mazo, *Welding International*, **28**: 557 (2014); https://doi.org/10.1080/09507116.2013.840042.
30. A. Unt, I. Poutiainen, S. Grünenwald, M. Sokolov, and A. Salminen, *Applied Sciences*, **7**, No. 12: 1276 (2017); https://doi.org/10.3390/app7121276.
31. I. L. Semenov, I. V. Krivtsun, and U. Reisgen, *Journal of Physics D: Applied Physics*, **49**, No. 10: 105204 (2016); https://doi.org/10.1088/0022-3727/49/10/105204.
32. D. Chinakhov, E. Chinakhova, S. Grichin, and Y. Gotovschik, *IOP Conference Series: Materials Science and Engineering*, **125**: 012013 (2016); https://doi.org/10.1088/1757-899X/125/1/012013.
33. D. Chinakhov and E. Agrenich, *Materials Science Forum*, **575**: 833 (2008); https://doi.org/10.4028/www.scientific.net/MSF.575-578.833.
34. H. Alipooramirabad, R. Ghomashchi, A. Paradowska, and M. Reid, *Journal of Materials Processing Technology*, **231**: 456 (2016); https://doi.org/10.1016/j.jmatprotec.2016.01.020.
35. H. Alipooramirabad, A. Paradowska, R. Ghomashchi, and M. Reid, *Journal of Manufacturing Processes*, **28**: 70 (2017); https://doi.org/10.1016/j.jmapro.2017.04.030.
36. J. C. F. Jorge, J. L. D. Monteiro, A. J. de Carvalho Gomes, I. de Souza Bott, L. F. G. de Souza, M. C. Mendes, and L. S. Araújo, *Journal of Materials Research and Technology*, **8**, Iss. 1: 561 (2019); https://doi.org/10.1016/j.jmrt.2018.05.007.